Full Text View

Volume 28, Issue 4 (April 1998)

Journal of Physical Oceanography

Article: pp. 563–576 | Abstract | PDF (147K)

Field Investigation of Transformation of the Wind Wave Frequency Spectrum with Fetch and the Stage of Development

Alexander V. Babanin and Yury P. Soloviev

Marine Hydrophysical Institute, Ukrainian National Academy of Sciences, Sevastopol, Crimea, Ukraine

(Manuscript received January 27, 1995, in final form June 23, 1997)

DOI: 10.1175/1520-0485(1998)028<0563:FIOTOT>2.0.CO;2

ABSTRACT

The variability of frequency spectra of waves is considered; for example, the dependencies of integral and spectral parameters of waves on wave-development factors and the interrelationships of the parameters are examined. Also studied is the transformation of the frequency spectrum shape in the course of its development, as well as the transition from the spectrum of developing waves to the spectrum of fully developed waves. Data were obtained in situ with common methods during a long-term program in the Black Sea.

The variability of the spectrum of developing waves, as a function of the stage of wave development, is described on the basis of field data using estimates of parameters for the spectrum form of the JONSWAP type. A novel approximation of the equilibrium interval level dependence on the dimensionless peak frequency $\bar{f}_m$ is obtained, which includes periods of stable and changeable behavior of the spectrum level. Transformation of the spectrum of wind-generated waves related to the development of the wave field in terms of the JONSWAP spectrum form is obtained. Continuous transition to the Pierson–Moskowitz spectrum is described. An approximation of the dependence of the enhancement coeffiecient γ on wave development stage $\bar{f}_m$ is suggested, which describes continuous variation of the coefficient γ for all wave ages. Self-similarity of the spectrum of developing waves is not observed.

Table of Contents:

1. Introduction

The study of dependency of the main wind wave parameters (like mean height and mean period) on conditions of their formation is based on traditional trend in wave investigations. At present there is no theory of wind wave spectral structure formation in the general case (Zakharov and Zaslavskii 1982a,b, 1983a,b). There are also substantial discrepancies not only between theoretical works of different authors but between results of estimating and generalizing field data as well (Davidan 1980). Thus, it is necessary to compare carefully results of the limited number of special experiments devoted to in situ wind wave research under controllable conditions.

According to the hypothesis of Kitaigorodskii (1970), the wind wave spectrum is fully determined by a limited number of parameters: frequency, wind velocity outside the boundary layer, duration of wind action, wave fetch, and gravitational acceleration. Ordinarily, wind speed at the standard height of 10 m is used for interpretation of field results.

Usually, groups of field data, even for such well-known experiments as JONSWAP (Hasselmann et al. 1973) have a rather narrow range of parameter variation that sets limits on the applicability of the obtained parameterizations. Sometimes, for construction of approximations, authors, in addition to their own data, must use data of other researchers obtained in other regions under various conditions, sometimes in laboratories and with different instrumentation. Such an approach may not always be correct and leads to degradation in accuracy of the resulting expressions.

The problem of using laboratory data for the analysis of wave spectral structure is of principal importance in wind wave experimental physics. The possibility of laboratory wave modeling should rather simplify research as far as it permits qualitative and quantitative studies of subtle effects. However, many theoretical and experimental studies indicate that the comparison of laboratory and field results needs extreme care. For example, Zaslavskii (1974) concluded that laboratory experiments are not representative of wave spectral structure because it is impossible to re-create the large-scale turbulence of the wind that plays a large role in wind wave growth. There are other important disadvantages of laboratory measurements; such as limited directional structure or involvement of capillary effects that restrict the resemblance of natural and laboratory waves too.

Thus, for reliable determination of the wind wave spectrum shape parameters (for example, on fetch), it is necessary to obtain a field dataset referring to as wide a range of values of the parameters as possible and, if possible, using similar instrumentation and common methods. The broadest well-known field dataset obtained within the scope of single research is a result of the special wave experiment of JONSWAP. However, the wide range of variation of dimensionless fetch $\tilde{X} = 10^2$–10^4 (see part 2) in this experiment is typical of the open sea and does not describe early stages of wave development. Among experiments devoted to the study of integral and spectral parameter variability, the studies of Kahma (1981), Donelan et al. (1985), Dobson et al. (1989), Wen et al. (1989), and Evans and Kibblewhite (1990) are distinguished by their comprehensive exploration of wind wave spectrum behavior based on field data obtained over a broad range of existing wave conditions. The present results will be compared with theirs as well as JONSWAP results.

For the study of integral and spectral wave parameter variations, systematic observations were carried out by the Department of Air–Sea Interaction, Marine Hydrophysical Institute of the Ukrainian National Academy of Sciences in 1981–89. Most data were acquired in the Black Sea (mainly, in its northwestern part), which is suitable for measuring developing seas and rather developed ones under controllable conditions of wave development (Fig. 1). The availability of stationary industrial (oil) rigs in the region provides an opportunity to perform long-term, in situ observations at a fixed point without the effect of motion on wave measuring instrumentation. The bottom relief is horizontally homogeneous and about 30 m deep, which satisfies deep sea conditions for typical waves in this region.

Measurements at a single fixed point, while actual conditions of wind and wave variations along the fetch are unknown, allow only indirect estimations of measurement conditions corresponding to “ideal” ones when the wind is steady, homogeneous, and perpendicular to the coastline. That is why only the following situations were chosen for further analysis:

1. The speed and direction of the wind were steady at least during the time interval from several to tens of hours.

2. The wind was directed within the range of 300°–120° (clockwise). Cases of prior turning or weakening of the wind were not considered.

An analysis of wind field maps for those cases shows that, under stationary conditions at $U > 5$ m s^{-1}, the horizontal scale of surface atmospheric structure essentially exceeds the dimensions of the measurement regions. Therefore, the wind field may be considered as approximately homogeneous and the distance to the coast in the direction of the wind is a good estimation of the fetch. The range of fetch variations was from 60 to 150 km.

Because only rather developed waves occur for steady wind that in the open sea regions, measurements from a stationary platform in the Black Sea nearshore zone (Katsiveli, Crimea’s South Coast) were acquired at the initial stages of wave development (Fig. 2). The wave fetches varied from 600 m to 1 km. The water depth at the platform is about 30 m, which implies deep water conditions for all short-fetched wave situations.

For wave measurements, a wire resistance wave gauge was mainly used, as described by Verkeev et al. (1983). The diameter of the nichrome string was ~ 0.3 mm, and its length 10 m. The device had been calibrated both in the laboratory and in situ. Laboratory tests demonstrated that the greatest deviation from linear regression between readings and water level never exceeded 1%, temperature-dependent errors in the range from 10° up to 30°C were less than 0.1%, and characteristics of the regression line changed no greater than 0.1% during a half-year. Field calibration (made by immersing the wires to various depths) showed ~ 1 mm accuracy for surface elevation. The platforms used to measure waves had eight 0.4-m diameter legs and, to avoid disturbance of the waves, the sensors were deployed on booms extended across the surface to a distance up to 15 m from the nearest leg. During measurements, only incident waves were recorded; that is, only waves unperturbed by the platform.

In some cases, an accelerometer wave buoy, as described by Babanin et al. (1993), was used. Its frequency response was investigated by comparison with simultaneous measurements made by a nearby wire gauge. Frequency spectra obtained with the buoy and the wire gauge coincided in all detail within 95% confidence interval up to 1.1 Hz.

To obtain directional characteristics of the wave field, we used arrays of string gauges. Characteristics of the arrays are described by Babanin and Soloviev (1987)and, for the purposes of the present paper, the main wave direction can be estimated with no greater than 10° accuracy.

Wave frequency spectra were obtained by a Fourier transform of a correlation function; frequency resolution was normally about 0.02 Hz; and the number of degrees of freedom was usually no less than 200. Directional spectra estimates were obtained by the maximum likelihood method (Capon 1969).

Simultaneous with wave measurements, continuous records of averaged wind speed and instantaneous direction were acquired once per minute. To measure the wind, a standard Russian M63-MP anemometer was used, it has a threshold of 0.5 m s^{-1}, and an accuracy of 0.05 V m s^{-1} for speed and 5° for direction where $V$is the measured wind speed. Anemometer data were recorded on a paper autoregister. To avoid flow distortions by the platform, anemometers were deployed on towers at 42 m height on the oil rigs and at 20 m height on the research platform at Katsiveli, far above the deck buildings. Speed and direction of the surface current, and water and air temperature were recorded once every three hours.

In most cases, the measurements of frequency spectra were coupled with directional spectra measurements by means of wave gauge arrays; thus, it is possible to choose “pure” situations with discrepancies between wind and wave directions of no more than 10°. This fact is of principal value because, in some recent studies (e.g., Donelan et al. 1985; Dobson et al. 1989), it has been noticed that, if a discrepancy exists between wind and wave directions at a measurement point, the proper wind to use in scaling wave parameters is the component of wind in the wave direction.

Though it is common practice to use in situ wind to scale the wave variables (Hasselmann et al. 1973; Donelan et al. 1985), some problems arise (Dobson et al. 1989). As the fetch profile of offshore wind changes due to variations of roughness length, the first question is what is the proper wind speed to use instead of that measured at a point because waves measured at the point are the product of the space and time history of the changing wind conditions all along the fetch. As shown by Dobson et al. (1989), corrections for scaling wind speed for initial fetches and for those greater than 50 km are small. The present data just fit both determined ranges; thus, the corrections described were not performed.

The second question is what offshore wind speed may be used for scaling at very short fetches, in sofar as the wind is strongly affected by the upwind presence of great roughness lengths. Here, there is no choice but measured wind speed because there are no clear criteria elaborated as to what properties should be considered characteristic for the wind at short fetches. If those are the properties of a wind suddenly started over a calm water surface, they will definitely differ from those of the offshore wind, but the former situation is much more exotic than the latter. Thus, to scale the wave variables at short fetches, the speed of the offshore wind was chosen. In all cases, the wind speed at the 10-m height used for scaling was not instantaneous but averaged over a period of the wave record, normally more than 15 min, and the situations chosen for analysis were always stationary.

2. Dependence of wave integral parameters on wave generation conditions

To cover a broad band of empirical parameters, Hasselmann et al. (1973), while constructing their dependencies, used, along with the data of the JONSWAP experiment, both field and laboratory data of other researchers. While plotting dimensionless wave spectrum peak frequency $\bar{f}_m = Uf_m/g$, where U is wind velocity at the 10-m height, f_m is dimensional spectrum peak frequency, and g is gravitational acceleration, versus dimensionless fetch $\bar{X} = gX/U^2$, where X is dimensional fetch, that generalization led to

$$\tilde{f}_m = 3.50\tilde{X}^{-0.33}. (1)$$

If laboratory data are eliminated and approximation parameters are determined only from JONSWAP data (Davidan 1980), another relation for $\tilde{f}_m$ and $\tilde{X}$ is obtained:

$$\tilde{f}_m = 2.55\tilde{X}^{-0.28}. (2)$$

The relation (2) differs essentially from the generalized approximation (1) (Fig. 3b). Significant discrepancies in the JONSWAP parameterization parameters obtained with and without the laboratory data were noted by Donelan et al. (1985), Dobson et al. (1989), and Donelan et al. (1993). The dependencies of Kahma (1981), Donelan et al. (1985), Dobson et al. (1989), Wen et al. (1989), and Evans and Kibblewhite (1990) are, after being expressed in a form similar to -(1), respectively

$$\tilde{f}_m = 3.18\tilde{X}^{-0.33}, \quad (3)$$

$$\tilde{f}_m = 1.85\tilde{X}^{-0.23}, \quad (4)$$

$$\tilde{f}_m = 1.7\tilde{X}^{-0.24}, \quad (5)$$

$$\tilde{f}_m = 1.66\tilde{X}^{-0.23}, \quad (6)$$

$$\tilde{f}_m = 2.98\tilde{X}^{-0.30}. \quad (7)$$

During data processing, after the analysis of atmospheric conditions, frequency spectra and directional wave features had been completed, 43 cases were chosen out of several hundreds of records to plot the peak frequency as a function of fetch. The cases correspond to steady wind waves with limited fetches (Table 1). The data were obtained using similar instrumentation within the framework of a common method of measurement and data processing.

Results (Fig. 3a) cover a wide range of wave conditions (from the earliest stages of wave development to stages close to fully developed). The range of wind speed variation covers velocities from 5 to 20 m s^{-1}. The ranges of dimensionless values were from 3×10^1 to 2×10^4 for fetch, from 10^{-5} to 10^{-3} for variance, from 0.84 to 0.18 for peak frequency. The main part of the data corresponds to fetches of 50–70 km and relates to developed and developing waves. The wave development stage parameter corresponding to these data is $U/c_m = 2\pi\tilde{f}_m = 1.0–1.7$, where c_m is the phase speed of a wave with frequency f_m. Field data related to young waves were very sparse. For that small group of data the parameter U/c_m was 3–5.

The approximation of the dependence of the dimensionless peak frequency on the dimensionless fetch is as follows:

$$\tilde{f}_m = [2.41^{+0.19}_{-0.18}]\tilde{X}^{-0.275\pm0.16}, (8)$$

which presents the 95% confidence interval of the empirical coefficients. This approximation is in good agreement (Fig. 3b) with the experimental dependencies of other authors, especially for developed waves. But only dependencies (2) and (3) fit the present dependency for young waves within 5% accuracy; the others differ by 10% or more.

The applicable range of the Zakharov–Zaslavskii spectrum (Zakharov and Zaslavskii 1982a,b, 1983a,b) is referred to as developed waves, and its comparison to experimental results can be carried out for the latest wave development stages only. In the range of developed waves with dimensionless fetches $\tilde{X} \sim 10^4$, the theoretical dependence of Zakharov and Zaslavskii (1983b)

$$\tilde{\omega}_m = 9.2\tilde{X}^{-3/14}$$

or

$$\tilde{f}_m = 1.46\tilde{X}^{-0.21}, \quad (9)$$

which agrees well with the experimental dependencies. It is particularly close to the results of Dobson et al. (1989) and Wen et al. (1989).

As noted above, according to the Kitaigorodskii's (1970) hypothesis, the wind speed U_0 on the outer side of boundary layer or the friction velocity u_* are among the few variables determining the wave spectrum. As measurements of the friction velocity u_* or the speed U_0 are of great difficulty, the mean wind speed U at the standard 10-m height is usually used for standardization of dimensionless values. Many authors (Davidan 1980; Efimov et al. 1986) considered such standardization to be not sufficiently correct as the wind speed U relates differently to the dynamic velocity u_* at different stages of wave development. On the other hand, in treating the energy containing part of the wave spectrum, Donelan et al. (1985) suppose that "since a significant proportion of the stress (Reynolds) is supported by very short waves, it would seem that the wind speed itself is more useful than the friction velocity as a means of characterizing the wind effects on the 'energy containing' gravity waves."

Thus, normalization based on the wind speed U at the standard 10-m height will be used here.

The peak frequency f_m is the most characteristic wave spectrum variable. It is weakly subjected to sampling variability, does not depend (unlike variance) on the long period modulation of wind waves (Efimov and Soloviev 1984), and varies slowly during the spectrum development (8). For the self-similar JONSWAP spectrum (Hasselmann et al. 1973), the peak frequency f_m, in general, determines the spectrum shape. Moreover, in field measurements, the peak frequency is the easiest variable to measure, unlike, for example, the wave fetch, which is usually unknown. Hence, assuming the dependence of the peak frequency on the wave fetch and the mean wind to be well described by the approximation (8), the relations between other parameters of the frequency spectrum shape and wave generation conditions will be considered in terms of their dependence on $\bar{f}_m$. To construct a dependence of the dimensionless variance

$$\bar{m} = \frac{mg^2}{U^4}$$

on the dimensionless peak frequency, 74 cases of stationary wave situations were chosen. The data are presented in Table 1. The resultant dependence is of the following form (Fig. 4):

$$\bar{m} = [8.30^{+2.46}_{-1.90}] \times 10^{-6}\bar{f}_m^{-(3.01\pm0.17)}, \quad (10)$$

where 95% confidence intervals for empirical coefficients are presented. Most of the variability in the dimensionless variance is caused by the variability of wind speed that enters into the dimensionless variance to the fourth power. Comparison of (10) with other approximations expressed in a form similar to ours are

Hasselmann et al. (1976):

$$\bar{m} = 5.1 \times 10^{-6}\bar{f}_m^{-10/3}, \quad (11)$$

Davidan (1980):

$$\tilde{\omega}_m = 0.11\bar{m}^{-0.34},$$

$$\bar{m} = 6.84 \times 10^{-6}\bar{f}_m^{-2.94}, \quad (12)$$

Kahma (1981):

$$\bar{m} = 1.16 \times 10^{-5}\bar{f}_m^{-3.00}, \quad (13)$$

Donelan et al. (1985):

Wen et al. (1989):

$$\tilde{m} = 7.693 \times 10^{-6}\tilde{f}_m^{-3.03}, \qquad (16)$$

Evans and Kibblewhite (1990):

$$\tilde{m} = 6.22 \times 10^{-6}\tilde{f}_m^{-2.91}, \qquad (17)$$

which demonstrates satisfactory coincidence (Fig. 4).

The theoretical dependence of Zakharov and Zaslavskii (1983b)

$$\tilde{m} = 1.5 \times 10^{-3}\tilde{\omega}_m^{-8/3} = 1.12 \times 10^{-5}\tilde{f}_m^{-2.67} \qquad (18)$$

also conforms satisfactory to empirical dependencies in the range of existence of the Zakharov–Zaslavskii spectrum but is more weak.

The good agreement of our results with those of other investigators suggests the universal character of the dependency describing variability of the peak frequency and the wave variance. Then the following questions arise:

1. is the spectrum behavior of universal character?
2. is the spectrum self-similar, as determined from the JONSWAP results (Hasselmann et al. 1973)?

3. Relation between spectrum shape parameters and integral wave parameters

Experimental verification of Kitaigorodsii's hypothesis resulted in the discovery of the Pierson–Moskowitz (PM) frequency spectrum (Pierson and Moskowitz 1964) for fully developed waves. The spectrum shape in the energy-containing frequency band (and at the forward face) was selected empirically, and as a result, the following PM spectrum form was established:

$$E_{PM}(f) = \alpha g^2 (2\pi)^{-4} f^{-5} \exp\left(-\frac{5}{4}(f/f_m)^{-4}\right), \qquad (19)$$

where $\alpha = 1.17 \times 10^{-2}$ determines the equilibrium interval level, g is the gravitational acceleration, and f_m is a spectral peak frequency. The dimensionless peak frequency and variance are constants:

$$\tilde{f}_m^{PM} = \frac{U f_m^{PM}}{g} \approx 0.13$$

$$\tilde{m}^{PM} = \frac{g^2 m^{PM}}{U^4} \approx 2.7 \times 10^{-3}. \qquad (20)$$

Because the PM spectrum applies to fully developed waves, the description of spectral characteristics for partially developed waves still remained unsolved. This problem was resolved as a result of the special international experiment, JONSWAP, conducted in 1968–69 in the North Sea (Hasselmann et al. 1973).

Among the results of the experiment, there was the modeling spectrum of developing waves. The JONSWAP spectrum has five parameters that not only depend on external conditions but are interdependent with each other:

$$\sigma_r = 0.09 \quad \text{for} \quad f > f_m,$$

where σ_l and σ_r describe the spectrum's (21) peak width from the left and right, respectively; and $\gamma = 3.3$ is an enhancement coefficient. The equilibrium interval level (α), in the JONSWAP spectrum does not remain constant [see (29)–(30)].

As one can see from (19) and (21), the JONSWAP spectrum differs from the PM spectrum by the value

$$\gamma^{\exp[(f-f_m)^2/(2\sigma^2 f_m^2)]}, \qquad (22)$$

which at $f = f_m$ is equal to the value of the enhancement coefficient $\gamma = 3.3$ and, while f recedes from f_m in either direction, the difference tends to unity rapidly. Thus, the spectrum (21) is very similar to the spectrum (19), only being narrower around the spectral peak. The main shortcoming resides in that the JONSWAP spectrum never transforms into the PM spectrum, that is, within the framework of this model, there is no transfer from the developing wave spectrum to the fully developed spectrum, although the JONSWAP data approaches fully developed situations.

To explain the last fact, Hasselmann et al. (1980) supposed that a rapid change occurs when waves approach their fully developed state. Such a shocklike spectrum change should be induced by corresponding shocklike change of the source functions. However, there is no evidence of similar jumps in the sources and, besides, the behavior of the terms responsible for the generation and nonlinear wave interactions is well known (e.g., Makin and Chalikov 1986; Komen et al. (1984)) and rather smooth. The empirical dependency on integral parameters also show persistent convergence the PM state (20) (Figs. 3 and 4), and an analogous dependency can be assumed for the spectral shape parameters; consequently, a smooth transition of a developing wave spectrum to the PM spectrum should occur.

Generally speaking, in spite of some shortcomings, especially those due to inclusion of laboratory data in the parameterization (Davidan 1980; Donelan et al. 1985; Dobson et al. 1989; Donelan et al. 1993), the JONSWAP spectrum is one of the most statistically well-founded empirical wind wave spectrum approximations known. Wind wave field spectra are well-described by the JONSWAP shape within the framework of statistical scattering, which is why the variability of the wind wave spectra are described here using the JONSWAP spectrum. The spectral width $\alpha$and the enhancement coefficient γ have the most scatter, the latter by a factor of 6 according to the JONSWAP data. In spite of such a wide range of variation, no evident tendency of their variability was found, so their average values were chosen for description of $\sigma$and γ in (21).

The JONSWAP spectrum shape was, to some degree, based on computations of nonlinear transfer in the balance equation. Because inputs of wind and dissipation in the energy-containing band of developed waves could be considered to be small, the slow evolution of the spectral peak must have been regulated by nonlinear interactions of wave components. Direct calculations of the one-dimensional nonlinear term demonstrated that the spectral shape (21) was optimal from the stability point of view because nonlinear interactions were a stabilizing mechanism that changed both narrower and wider spectra, leading to the JONSWAP shape. After a spectral shape had become stable, Eq. (21), it did not vary further, and the spectrum evolved slowly due to energy input of the wind in the short-wave band and nonlinear interaction transfer to the long-wave band, where the spectral peak moved to lower frequency and, accordingly, its spectral density grew. The scatter in field data for spectral shape parameters σ and γ was considered to be natural and is explained by the small-scale nonhomogeneity of the wind field.

Notwithstanding the convenience of the arguments, the existence of stable wind wave field spectra much wider than the JONSWAP spectrum is an experimental fact. The PM spectrum is statistically well assured and is obtained as the steady state spectrum for a wide range of wind speeds from 10 to 40 m s^{-1}. Komen et al. (1984) investigated conditions of the balance equation for the PM equilibrium spectrum to exist. Accounting for the two-dimensionality of wave spectra allows one to explain the stability of the one-dimensional (frequency) PM spectrum as the steady-state frequency spectrum.

Thus, the transition from the narrow frequency spectrum of developing waves to the wide spectrum of fully developed waves should be smooth. To describe this parametrically, there is no need to abandon empirical approximations (21) and (19); it is sufficient to assume that the dependence of the enhancement coefficient γon the wave development stage had been accounted for in natural data scatter. If spectral enhancement is assumed to decrease gradually during wave development and that $\gamma = 1$ for the spectrum of fully developed waves, the necessary transition between spectra (21)and (19) will be achieved.

To investigate the dependence of the developing wave spectrum on the wave development stage, estimations of spectral shape parameters of the JONSWAP type were conducted on the basis of field data obtained in the Black Sea.

For analysis of spectral width, the following width definition suggested by Belberov et al. (1983) was used:

$$\nu = \frac{m}{\omega_m E(\omega_m)}. \qquad (23)$$

The parameter $\nu = \Delta\omega/\omega_m$ may be interpreted as a relative width of a rectangular spectrum having an area, m and a central frequency ω_m. Soloviev (1989) demonstrated that value of ν is $\nu_{PM} = 0.698$ for the PM spectrum and $\nu_J = 0.323$ for the JONSWAP spectrum.

The dependence of spectral width ν on dimensionless frequency $\tilde{f}_m$ as a parameter of wave development stage was obtained by Krivinskii (1991):

$$\nu = \begin{cases} (1.05 \pm 0.02) - (2.49 \pm 0.13)\tilde{f}_m \quad \text{for } \tilde{f}_m \le 0.29 & (24a) \\ 0.323 \quad \text{for } \tilde{f}_m > 0.29. & (24b) \end{cases}$$

As seen from (24), the spectral width ν (23) remains constant until a certain wave development stage ($U/c_m = 2\pi\tilde{f}_m = 1.8$, $\tilde{f}_m = 0.13$) has been reached; then the spectrum starts to widen and reaches the PM value.

Special investigations of field spectra were carried out to study the behavior of the equilibrium interval. The level α, of the equilibrium interval was determined in the same way as by other authors (Bandou et al. 1986); the data are listed in Table 2. In general, 58 spectra obtained at different wave development stages were used. As seen in Fig. 5 the data are separable into two groups. For developed waves ($U/c_m \approx 0.8 - 2$), the strong dependence of level α on wave age parameter $\tilde{f}_m$ is observed. The spectral density level in the equilibrium interval, away from the fully developed wave stage, essentially rises. However, this tendency is not supported by spectra of young waves since for $U/c_m > 3$ the Phillips parameter α has the same values as those for $U/c_m \sim 2$. Data in the intermediate region, are not available. The approximation of the parameter α dependence on wave development stage $\tilde{f}_m$ has the following form:

$$\alpha = \begin{cases} (8.03^{+0.57}_{-0.54})10^{-2}\tilde{f}_m^{1.24\pm0.23} \quad \text{for } \tilde{f}_m \le 0.23 & (25a) \\ 13.2 \times 10^{-3} \quad \text{for } \tilde{f}_m > 0.23. & (25b) \end{cases}$$

For the empirical coefficients, the 95% confidence intervals are presented. At a constant level for young waves, the value close to the one assumed by Phillips (1966) is chosen in (25b). In the range (25a), the equilibrium level changes gradually from 7.07×10^{-3} at $\tilde{f}^{PM}_m = 0.13$, close to the PM constant $\alpha_{PM} = 8.1 \times 10^{-3}$, up to the (25b) level. The two ranges of (25) are in good agreement with ranges of spectral width (ν) variability in (24).

The function (25) is shown, in Fig. 5, together with the empirical approximations of Hasselmann et al. (1973), Bandou et al. (1986), Donelan et al. (1985), and Evans and Kibblewhite (1990). Empirical points below the PM frequency $\tilde{f}^{PM}_m = 0.13$ were not used for approximation (25) because there can be several possible explanations of their appearance; for example, violation of the wind field homogeneity along fetch under low values of local wind speed, effects of atmospheric stability variability along the fetch, occurence of a variety of wave-induced drag mechanisms at different fetches, etc.

The functions of Donelan et al. (1985)

$$\alpha = 0.006\left(\frac{U}{c_m}\right)0.55 = 1.65 \times 10^{-2}\tilde{f}_m^{0.55} \qquad (26)$$

and Evans and Kibblewhite (1990)

$$\alpha = 2.4 \times 10^{-2}\tilde{f}^{0.833}_m (27)$$

are attempts at construction of joint lines for all development stages. Those lines would coincide well with the function (25) if the present data had not been split into two ranges and then fit with a joint approximation, but a similar dependence would give significant errors due to the quantitatively incorrect behavior in the middle region of the wave development stages.

The approximation of Bandou et al. (1986) obtained in a laboratory tank is the next form considered after scaling by the wind speed adjusted to the 10-m height:

$$\alpha = 3.26 \times 10^{-2} \tilde{f}_m^{6/7}. \quad (28)$$

The problem with using laboratory data for the analysis of wave spectral structure laws was already discussed in section 1. The different conditions of wind wave generation in the field and laboratory situations can lead to weak similarity to laboratory data. The dependence (28) has intermediate behavior compared (Fig. 5) with the field dependencies (25), (26), and (27) in the main range of wave development.

The importance of the problem of combined laboratory and field data usage is well understood from the discussion of JONSWAP results. As already mentioned, to study the spectral shape variability in as broad as possible set of conditions Hasselmann et al. (1973) used, together with the data of JONSWAP itself, results of other researchers, including the laboratory data. Finally, the following dependence of the parameter α on the dimensionless fetch $\tilde{X} = Xg/U^2$ was obtained:

$$\alpha = 0.076 \tilde{X}^{-0.22}. \quad (29)$$

The analogous connection of α and $\tilde{X}$ using only data of the JONSWAP experiment differs essentially:

$$\alpha \sim \tilde{X}^{-0.4}. \quad (30)$$

After recalculation of (29) and (30) for dimensionless frequency using (8), the following are obtained:

$$\alpha = 3.76 \times 10^{-2} \tilde{f}_m^{0.80} \quad (31)$$

and

$$\alpha \sim \tilde{f}_m^{1.45}. \quad (32)$$

The first approximation constructed using data at all wave development stages agrees well with (28) by Bandou et al. (1986), and the second approximation coincides better in its slope with (25a) corresponding to the range describing well-developed waves. Taking into account that data obtained at the early development stages are not represented in the JONSWAP dataset, the general agreement of (25a) and (32) indicates a good confirmation of the approximation (25a).

Another indirect but clear confirmation of (25) may be found in Evans and Kibblewhite (1990), who noted for the equilibrium range that "the spectrum level increases up to wind speeds of 15 m s^{-1} at which stage the spectrum levels for higher wind speeds tend to merge." According to Fig. 3 of Evans and Kibblewhite (1990), this wind speed corresponds to $\tilde{f}_m = 0.23$, which is exactly our transition dimensionless frequency. A desire to construct a continuous dependence using all wave conditions together leads to the smoothed approximations (26), (27), and (31).

The described results demonstrate the existence of two different phases of wind wave development. During the first phase, for young waves, the level of equilibrium interval α is described by $\alpha = 1.32 \times 10^{-2}$, and the spectrum width ν (Krivinskii 1991) remains constant, equal to the JONSWAP spectrum width. During the second phase, for developed waves, the level α varies from those values corresponding to the spectrum of developing waves down to values of the PM spectrum, and the width ν (according to Krivinskii 1991) varies in a similar way too.

4. Transformation of wave frequency spectrum

In the previous part, the dependencies of wind wave spectral shape parameters on wave generation conditions have been considered. In the JONSWAP spectrum, the parameters vary in such a way that their spectrum is self-similar, its shape remains invariant, and the spectrum is determined by the peak frequency f_m. Under such a construction, it is necessary to include a discontinuity of the self-similarity at a definite stage to describe the transition from the JONSWAP developing wave spectrum to the PM spectrum of fully developed waves.

Hasselmann et al. (1973) suggested a criterion for the JONSWAP spectrum self-similarity. If the spectrum shape (21) is maintained, the relation is fulfilled for the dimensionless energy $\tilde{m} = mg^2/U^4$:

$$\tilde{m} \sim \alpha \tilde{f}_m^{-4}. \quad (33)$$

The dependencies of JONSWAP for the equilibrium interval α and the dimensionless peak frequency $\tilde{f}_m = Uf_m/g$ on the dimensionless fetch $\tilde{X} = Xg/U^4$ were already written in (29) and (1). The empirical approximation of JONSWAP for the connection of the variance $\tilde{m}$ and the fetch $\tilde{X}$ has the following form:

$$\tilde{m} = 1.6 \times 10^{-7} \tilde{X}. \quad (34)$$

If the expression (29) is fulfilled, the parameter λ will be the criterion of self-similarity:

$$\lambda = \frac{\tilde{m}\tilde{f}_m^4}{\alpha}. \quad (35)$$

This parameter should remain constant. As it follows from (1), (29), (34) (see Hasselmann et al. 1973):

$$\lambda \sim \tilde{X}^{4(-0.33)+1-(-0.22)} = \tilde{X}^{-0.1}. \quad (36)$$

Within the JONSWAP data error bounds

$$\lambda = 1.62 \times 10^{-4}. \quad (37)$$

It has already been mentioned that the JONSWAP spectrum shape was assumed to be self-similar, but possible departures from (36) would lead to alterations of the JONSWAP spectral shape.

The dependence of λ on the dimensionless peak frequency $\tilde{f}_m$ was obtained for the field spectra in the Black Sea (Fig. 6 and Table 2). The strong natural scatter of experimental points does not allow construction of a reliable approximate functional dependence between $\lambda$and $\tilde{f}_m$, though obvious trends indicate that the parameter does not remain constant. The average λ value in the interval $\tilde{f}_m < 0.23$ of developed waves is

$$\lambda = (1.60 \pm 0.55) \times 10^{-4}, \quad (38)$$

which agrees well with the JONSWAP results (37). In the interval $\tilde{f}_m > 0.23$,

$$\lambda = (2.42 \pm 1.06) \times 10^{-4}, \quad (39)$$

which is quite different from (37).

Thus, the behavior of λ does not give clear evidence to support the statement of self-similarity for the JONSWAP spectrum. Besides, as anticipated and will be seen further, other JONSWAP spectrum parameters, such as the enhancement coefficient γ, are involved in differences so that λ does not have a clear physical sense, which was attributed to it by Hasselmann et al. (1976). As can easily be shown, the JONSWAP enhancement coefficient γ is connected with other JONSWAP spectral parameters and the spectral width ν as follows:

$$\gamma = (2\pi)^4 e^{5/4} \frac{\tilde{m}\tilde{f}_m^4}{\alpha\nu}. \quad (40)$$

The expression (40) allows computation of the γ dependence using dependency on the spectral width ν and the parameters $\tilde{m}$, $\tilde{f}_m$, and α. The large natural scatter of the enhancement coefficient does not allow construction of the dependence of γ on wave development stage $\tilde{f}_m$ by means of the experimental data, though treatment of γ as a constant, as Hasselmann et al. (1973) did, is clearly unsuitable.

For the convenience of estimating γ, the dependence of the width ν on the dimensionless frequency $\tilde{f}_m$ was recalculated as a power function, using the same experimental dataset used by Krivinskii (1991) to construct the linear approximation (24):

$$\nu = \begin{cases} (0.118^{+0.066}_{-0.043})\tilde{f}_m^{-0.91\pm0.30}, & \text{for } \tilde{f}_m \le 0.23, \quad (41a) \\ 0.449, & \text{for } \tilde{f}_m > 0.23. \quad (41b) \end{cases}$$

Such dependence does not yield the linear relation (24a) according to the statistical scatter minimum criterion. As in the case of (25), the frequency $\tilde{f}_m = 0.23$ was chosen as a transition though now it corresponds to a somewhat wider spectrum than the JONSWAP spectrum (24b).

The variability of the enhancement coefficient's dependence on the wave development stage, $\tilde{f}_m$, is now calculated. During the first period of wave growth, for $\tilde{f}_m > 0.29$, the calculated dependence for γ has the following form:

$$\gamma = [7.62^{+2.38}_{-1.75}]\tilde{f}_m^{0.99\pm0.17} \approx 7.6\tilde{f}_m. \quad (42)$$

The last approach was chosen, in the framework of confidence intervals, for γ to become unity if the dependence continued to the frequency $\tilde{f}_m = \tilde{f}^{PM}_m = 0.13$.

In the range of developed waves, $0.13 \leqslant \tilde{f}_m \leqslant 0.23$

$$\gamma = [4.75^{+8.95}_{-6.64}]\tilde{f}_m^{0.66\pm0.70} \approx 7.6\tilde{f}_m. \quad (43)$$

Here, the dependence is not statistically reliable, and the approximating function was chosen inside the confidence intervals to reach unity at $\tilde{f}_m = \tilde{f}^{PM}_m = 0.13$, and as a continuation of the dependence (42) obtained reliably for the developing waves. Thus, the enhancement, coefficient γ does not remain constant, as assumed in Hasselmann et al. (1973). The final dependence is based on continuity from both above and below the wave stage $\tilde{f}_m = 0.23$:

$$\gamma \approx 7.6\tilde{f}_m. \quad (44)$$

Among the parameters of the JONSWAP spectrum shape (21), the spectral peak width, σ, does not remain constant either. Its dependence on the wave development stage is determined completely by the variability of the width ν (24) and the enhancement coefficient γ (44) and is not considered further here as it is not of independent interest and cannot be directly obtained.

5. Discussion and conclusions

The calculation of the dependence of the enhancement coefficient γ of the JONSWAP-type spectrum (21) on wave development stage demonstrates that coefficient γ decreases according to a definite law (44) as the waves grow. The corresponding spectrum, having the JONSWAP shape (21), though with the varying coefficients γ and σ, varies in such a way that for the dimensionless frequency $\tilde{f}_m = 0.13$ determined by Pierson and Moskowitz (1964) as a limiting value for wind waves, it merges into the PM spectrum of fully developed waves. The coefficient γ reaches the mean JONSWAP value $\gamma_J = 3.3$ for $\tilde{f}_m = 0.43$, which corresponds to an intermediate wave development stage.

Another description of the transition from the narrow, fetch-limited spectrum to the broad fully developed spectrum was presented by Donelan et al. (1985). Generally, they retained the JONSWAP spectrum shape but introduced the −4 power law for the rear face of the spectrum. Their well-established spectrum is in reasonable agreement with the JONSWAP spectrum for young waves and approaches the PM spectrum for fully developed waves. To move forward in this direction, the problem of the behavior of the wave spectral equilibrium interval is probably of significant importance.

The dependence (44) is only statistically averaged, there is a large scatter of individual γ values relative to the average dependence. As shown by Hasselmann et al. (1973), such scatter may be recognized as natural and connected with the local instability of the wind field, that is, with its gustiness. The great scatter of the parameters of the spectrum peak shape is considered a disadvantage of the JONSWAP model (21) of the wind wave spectrum, but here the aim was not to remove this disadvantage and propose a different spectrum. Instead, the lack of description of the spectrum development was attempted in the framework of the well-established JONSWAP form. Physical reasons for alterations of the wave frequency spectra at temporal scales of tens of minutes are still open to discussion.

As a result, the transformation of the frequency spectrum during its development is described by means of the variations of the set of the parameters of the JONSWAP spectrum shape—the statistically well-established approximation of the in situ field spectra. The dependencies of the wave energy $\tilde{m}$, and the spectrum peak shape parameter γ on the dimensionless frequency $\bar{f}_m$ are universal and do not vary as the different wave development stages occur. During the first stage of wave development the equilibrium interval level, α and the relative spectrum width ν remain constant. For developed waves, the level α decreases and the relative width ν increases.

Limitations of these conclusions have two major sources: the lack of data at the intermediate wave fetches and the great scatter of the parameters of the JONSWAP spectrum shape. The former limitation, though may lead to some improvements if the data are obtained, but it is assumed to not cause sharp changes in the dependencies because their behavior in the missed ranges seems to be rather smooth. However, natural scatter imposes serious questions on the suppositions and explanations made. Though achieved with high accuracy and well-proven statistically, the measurements still demonstrate that scatter of the spectral parameters, caused apparently by natural geophysical variability, leads individual wave spectra sometimes far beyond average assumed shapes.

The present dataset was measured with high accuracy, thoroughly processed, and verified to meet both demands to fit pure conditions of wave generation and to cover a broad range of wave development stages. Dependency of integral wave parameters on wind wave conditions demonstrate that the observed data fit final expressions with high correlation. The scattering of spectral shape parameters around average dependencies that appears to be of large magnitude leads to the conjecture that further improvement of the description of spectral development is related not to more accurate measurements or more comprehensive datasets but to an accounting for wind and wave variability properties instead of average characteristics obtained accurately in our experiments.

In such a way, the description of the wind wave spectrum transformation with the wave system development is obtained in terms of the JONSWAP spectrum shape parameters. The self-similarity of the developing wave spectrum is not observed, and the permanent modification of the spectrum shape, dependent on the wave age, occurs. In the framework of the JONSWAP spectrum shape, a continuous transition from the narrow spectrum for developing waves to the wide spectrum for fully developed waves of Pierson–Moskowitz is obtained.

Acknowledgments

The authors would like to express their appreciations to V. G. Proshchenko, P. P. Verkeev, and A. I. Korovushkin for their aid with the experiments, and to Prof. V. V. Efimov for useful discussions. We express particular gratitude to our editor Prof. C. N. K. Mooers and our unknown reviewers whose remarks helped us improve the final version of the paper.

REFERENCES

Babanin, A. V., and Y. P. Soloviev, 1987: Parameterization of the width of angular distribution of the wind wave energy at limited fetches (in Russian, English abstract), *Izv. Akad. Nauk SSSR, Fiz. Atmos. Okeana,* **23,** 868–876..

— ,P. P. Verkeev, B. B. Krivinskii, and V. G. Proshchenko, 1993: Measurement of wind waves by means of a buoy accelerometer wave gauge. *Phys. Oceanogr.,* **4,** 387–393..

Bandou, T., H. Mitsuyasu, and T. Kusaba, 1986: An experimental study of wind waves and low frequency oscillations of water surface. *Reports of Research Institute for Applied Mechanics,***XXXIII,** 13–32..

Belberov, Z. K., V. M. Zhurbas, M. M. Zaslavskii, and L. G. Lobisheva, 1983: Integral characteristics of wind wave frequency spectra. *Interaction of Atmosphere, Hydrosphere, and Litosphere in Near-Shore Zone of the Sea* (in Russian, English summary), Z. Belberov, V. Zahariev, O. Kuznetsov, N. Pykhov, B. Filyushkin, and M. Zaslavskii, Eds., Bulgarian Academy of Science Press, 143–154..

Capon, J., 1969: High-resolution, frequency–wavenumber, spectrum analysis. *Proc. IEEE,* **57,** 1408–1418..

Davidan, I. N., 1980: Investigation of wave probability structure on field data. *Trudi* (in Russian). *GOIN,* **151,** 8–26..

Dobson, F., W. Perrie, and B. Toulany, 1989: On the deep-water fetch laws for wind-generated surface gravity waves. *Atmos.–Ocean,***27,** 210–236..

Donelan, M. A., J. Hamilton, and W. H. Hui, 1985: Directional spectra of wind-generated waves. *Philos. Trans. Roy. Soc. London, Ser. A,* **315,** 509–562..

— , F. W. Dobson, S. D. Smith, and R. J. Anderson, 1993: On the dependence of sea surface roughness on wave development. *J. Phys. Oceanogr.,* **23,** 2143–2149..

Efimov, V. V., and Y. P. Soloviev, 1984: Low-frequency oscillations of sea level and group structure of wind waves (in Russian, English abstract). *Izv. Akad. Nauk SSSR, Fiz. Atmos. Okeana* **20,**985–994..

— , B. B. Krivinskii, and Y. P. Soloviev, 1986: Study of the energetic sea wind waves fetch dependence (in Russian, English abstract). *Meteor. Gidrol.,* **11,** 68–75..

Evans, K. C., and A. C. Kibblewhite, 1990: An examination of fetch-limited wave growth off the west coast of New Zealand by a comparison with the JONSWAP results. *J. Phys. Oceanogr.,* **20,**1278–1296..

Hasselmann, D. E., M. Dunckel, and J. A. Ewing, 1980: Directional wave spectra observed during JONSWAP 1973. *J. Phys. Oceanogr.,* **10,** 1264–1280..

Hasselmann, K., T. P. Barnett, E. Bouws, H. Carlson, D. E. Cartwright, K. Enke, J. A. Ewing, H. Gienapp, D. E. Hasselmann, P. Kruseman, A. Meerburg, P. Muller, D. J. Olbers, K. Richter, W. Sell, and H. Walden, 1973: Measurement of wind wave growth and swell decay during the Joint North Sea Wave Project (JONSWAP). Dtsch. Hydrogr. Instit., 95 pp..

— , D. B. Ross, P. Muller, and W. Sell, 1976: A parametric wave prediction model. *J. Phys. Ocenogr.,* **6,** 200–228..

Kahma, K. K., 1981: A study of the growth of the wave spectrum with fetch. *J. Phys. Oceanogr.,* **11,** 1503–1515..

Kitaigorodskii, S. A., 1970: *Physics of Atmosphere and Ocean Interaction* (in Russian). Gidrometeoizdat, 284 pp..

Komen, G. I., S. Hasselmann, and K. Hasselmann, 1984: On the existence of a fully developed wind-sea spectrum. *J. Phys. Oceanogr.,* **14,** 1271–1285..

Krivinskii, B. B., 1991: Variability of energetic characteristics of wind surface waves (in Russian). Ph.D. dissertation, Marine Hydrophysical Institute, Ukrainian National Academy of Sciences, 191 pp..

Makin, V. K., and D. V. Chalikov, 1986: The calculation of impulse and energy flows to developing waves. *Izv. Akad. Nauk SSSR, Fizika Atmos. Okeana,* **22,** 1309–1316..

Phillips, O. M., 1966: *The Dynamics of the Upper Ocean.* Cambridge University Press, 261 pp..

Pierson, W. J., Jr., and L. Moskowitz, 1964: A proposed spectral form for fully developed wind seas based on the similarity theory of S. A. Kitaigorodskii. *J. Geophys. Res.,* **69,** 5181–5190..

Soloviev, Y. P., 1989: Modelling of wind wave envelope spectral characteristics. *Mar. Hydrophys. J.* **2,** 27–33..

Verkeev, P. P., A. I. Korovushkin, B. B. Krivinskii, V. G. Proshchenko, and Y. P. Soloviev, 1983: Methods and equipment for measurements of parameters of wind-generated and internal waves. *Experimental and Theoretical Research of Air–Ocean Interaction*(in Russian), Sevastopol, 34–44..

Wen, S. C., D. C. Zhang, P. Z. Guo, and B. H. Chen, 1989: Parameters in wind–wave frequency spectra and their bearings on spectrum forms and growth. *Acta Oceanol. Sinica,* **8,** 15–39..

Zakharov, V. E., and M. M. Zaslavskii, 1982a: Kinetic equation and Kolmogorov's spectra in a week turbulence theory of wind waves. *Izv. Akad. Nauk SSSR, Fiz. Atmos. Okeana,* **18,** 970–979..

— , and — , 1982b: Integrals of wind input and dissipation in kinetic equation of a weak turbulence theory of wind waves. *Izv. Akad. Nauk SSSR, Fiz. Atmos. Okeana,* **18,** 1066–1076..

— , and — , 1983a: The shape of the spectrum of energy containing components of the water surface in the weakly turbulent theory of wind waves. *Izv. Akad. Nauk SSSR. Fiz. Atmos. Okeana,* **19,** 282–291..

— , and — , 1983b: The dependence of wave parameters on wind velocity, its duration and fetch in a weak turbulence theory of wind waves. *Izv. Akad. Nauk SSSR, Fiz. Atmos. Okeana,* **19,**406–415..

Zaslavskii, M. M., 1974: To the theory of surface waves and turbulence boundary atmosphere layer interaction. *Izv. Akad. Nauk SSSR, Fiz. Atmos. Okeana*, **10,** 1282–1292..

Tables

Table 1. Wind and wave characteristics used for construction of the integral dependencies.

No. 1	U (m s^{-1}) 2	u_* (m s^{-1}) 3	f_m (Hz) 4	$\tilde{f}_m$ 5	$\tilde{f}^*_m \times 10^3$ 6	m (m^2) 7	$\tilde{m} \times 10^4$ 8	$\tilde{m}^* = \frac{mg^2}{u_*^4}$ 9	X (km) 10	$\tilde{X}$ 11	$\tilde{X}^* \times 10^{-6}$ 12
1	9.15	0.317	0.78	0.73	25.3	0.0009	0.13	8.96	0.67	78.5	0.066
2	7.0	0.23	0.83	0.59	19.6	0.0006	0.26	21.0	0.67	134.0	0.124
3	11.8	0.474	0.70	0.84	33.8	0.0023	0.12	4.4	0.90	63.7	0.032
4	10.4	0.384	0.68	0.73	26.7	0.0022	0.18	9.6	0.84	75.7	0.056
5	11.7	0.168	0.22	0.26	10.4	0.112	5.75	225	50.8	3640	2.28
6	11.6	0.461	0.20	0.24	9.4	0.140	7.44	298	52.0	3790	2.40
7	11.9	0.483	0.20	0.24	9.8	0.181	8.69	320	54.6	3780	2.30
8	11.7	0.468	0.20	0.24	9.5	0.127	6.52	255	54.6	3190	2.45
9	11.5	0.454	0.20	0.23	9.3	0.155	8.53	351	56.1	4160	2.67
10	11.3	0.440	0.20	0.23	9.0	0.153	9.03	393	57.7	4430	2.92
11	10.6	0.394	0.20	0.22	8.0	0.126	9.60	503	54.6	4770	3.45
12	10.6	0.394	0.20	0.22	8.0	0.120	9.14	479	54.6	4770	3.45
13	10.6	0.394	0.22	0.23	8.7	0.120	9.15	479	54.6	4770	3.45
14	12.4	0.521	0.18	0.23	9.7	0.235	9.57	307	54.6	3480	1.97
15	12.4	0.521	0.19	0.24	1.0	0.210	8.55	274	54.6	3480	1.97
16	10.6	0.394	0.19	0.21	7.7	0.145	11.05	579	50.0	4370	3.16
17	10.6	0.394	0.23	0.25	9.4	0.078	5.95	311	49.6	4330	3.13
18	13.6	0.615	0.175	0.24	11.0	0.500	14.1	337	150	7960	3.89
19	17.8	0.552	0.175	0.23	9.9	0.430	15.4	445	140	8380	4.50
20	15.1	0.724	0.175	0.27	12.0	0.379	7.02	132	61.8	2660	1.15
21	10.0	0.360	0.20	0.20	7.34	0.107	10.3	613	110	10 800	8.33
22	10.1	0.364	0.18	0.185	6.68	0.105	9.71	576	110	10 600	8.14
23	9.8	0.349	0.19	0.19	6.76	0.098	10.2	637	110	11 200	8.86
24	6.35	0.108	0.20	0.13	4.24	0.049	28.8	2500	110	26 800	24.9
25	6.2	0.202	0.22	0.14	4.53	0.042	27.1	2400	118	28 800	28.4
26	13.9	0.638	0.20	0.28	13.0	0.192	4.95	112	53.3	2710	1.28
27	9.3	0.324	0.22	0.21	7.27	0.089	11.4	776	59.8	6800	5.59
28	11.4	0.447	0.20	0.23	9.11	0.169	9.63	407	110	4830	9.40
29	13.0	0.568	0.19	0.25	11.0	0.164	5.53	151	67.5	3720	2.06
30	15.6	0.757	0.20	0.32	15.4	0.215	3.49	63	61.1	2410	1.05
31	10.1	0.365	0.18	0.185	6.70	0.121	11.2	656	110	6150	8.10
32	10.1	0.365	0.18	0.185	6.70	0.118	10.9	640	110	6150	8.10
33	9.8	0.349	0.19	0.19	6.76	0.086	8.88	555	110	11 200	8.86
34	10.1	0.365	0.18	0.185	6.70	0.086	7.76	455	110	10 600	8.10
35	6.4	0.208	0.20	0.13	4.24	0.045	26.5	2310	110	26 800	24.9
36	6.5	0.213	0.21	0.14	4.56	0.035	18.6	1610	110	25 500	23.8
37	9.3	0.324	0.24	0.23	7.93	0.050	6.44	438	59.8	6780	5.59
38	9.3	0.324	0.24	0.23	7.93	0.072	9.31	632	59.8	6780	5.59
39	9.2	0.317	0.27	0.25	8.7	0.0431	5.80	412	62.4	7230	6.09
40	9.0	0.309	0.23	0.21	7.2	0.039	5.73	413	62.4	7560	6.41
41	11.4	0.447	0.20	0.23	9.1	0.129	7.35	311	110	8300	5.40
42	8.7	0.298	0.24	0.21	7.3	0.046	7.73	561	7.0	9080	7.73
43	15.9	0.777	0.56	0.91	44.4	0.0096	0.15	2.5	840	32.6	0.014
44	5.2	0.169	0.42	0.22	7.24	0.013	17.1	1530	—	—	—
45	6.7	0.220	0.28	0.19	6.28	0.050	23.7	2040	—	—	—
46	11.1	0.424	0.20	0.23	8.64	0.048	3.02	142	—	—	—
47	10.1	0.363	0.17	0.175	6.29	0.163	15.1	903	—	—	—
48	10.2	0.368	0.15	0.16	5.63	0.094	8.33	492	—	—	—
49	11.1	0.424	0.15	0.17	6.48	0.142	9.00	423	—	—	—
50	7.9	0.266	0.17	0.14	4.61	0.083	20.4	1590	—	—	—
51	4.9	0.158	0.22	0.11	3.54	0.013	21.9	2020	—	—	—
52	6.6	0.218	0.27	0.18	6.00	0.037	18.8	1580	—	—	—
53	6.5	0.211	0.23	0.15	4.95	0.044	23.6	2130	—	—	—
54	6.9	0.228	0.23	0.16	5.35	0.058	24.7	2070	—	—	—
55	6.9	0.228	0.23	0.16	5.35	0.039	16.4	1370	—	—	—
56	7.1	0.234	0.23	0.17	5.49	0.040	15.1	1280	—	—	—
57	6.7	0.221	0.25	0.17	5.63	0.051	24.4	2060	—	—	—
58	7.5	0.248	0.23	0.18	5.81	0.048	14.5	1220	—	—	—
59	7.8	0.258	0.25	0.20	5.67	0.034	8.81	736	—	—	—
60	8.8	0.300	0.25	0.22	7.65	0.050	7.84	588	—	—	—
61	9.2	0.320	0.25	0.23	8.15	0.084	11.3	773	—	—	—

Click on thumbnail for full-sized image.

Table 1. *(Continued)*

No. 1	U (m s^{-1}) 2	u_* (m s^{-1}) 3	f_m (Hz) 4	$\tilde{f}_m$ 5	$\tilde{f}^*_m \times 10^3$ 6	m (m^2) 7	$\tilde{m} \times 10^4$ 8	$\tilde{m}^* = \frac{mg^2}{u_*^4}$ 9	X (km) 10	$\tilde{X}$ 11	$\tilde{X}^* \times 10^{-6}$ 12
62	10.8	0.410	0.27	0.30	11.3	0.110	7.78	375	—	—	—
63	12.2	0.502	0.20	0.25	10.2	0.056	2.42	85	—	—	—
64	6.8	0.224	0.16	0.11	3.65	0.065	29.1	2470	—	—	—
65	12.4	0.521	0.12	0.15	6.36	0.154	6.27	201	—	—	—
66	13.3	0.590	0.12	0.16	7.22	0.196	6.03	156	—	—	—
67	6.8	0.224	0.18	0.125	4.12	0.081	36.5	3100	—	—	—
68	13.9	0.639	0.20	0.281	13.0	0.192	4.5	111	—	—	—
69	6.6	0.217	0.35	0.231	7.74	0.006	3.09	264	—	—	—
70	4.8	0.157	0.33	0.161	.28	0.007	12.4	1090	—	—	—
71	5.0	0.163	0.35	0.180	.82	0.007	10.1	896	—	—	—
72	7.9	0.262	0.30	0.240	8.01	0.012	3.22	253	—	—	—
73	5.2	0.169	0.32	0.17	5.51	0.011	14.2	1280	—	—	—
74	4.7	0.153	0.30	0.14	4.68	0.009	18.2	1620	—	—	—

Click on thumbnail for full-sized image.

Table 2. Wind and wave characteristics and JONSWAP-type spectrum shape parameters used to construct the spectrum parameter dependencies.

	U (m s^{-1})	f_m (Hz)	$\tilde{f}_m$	m (m^2)	$\alpha \times 10^3$	$\lambda \times 10^2$
1	15.1	0.175	0.269	0.379	14.40	2.57
2	4.6	0.52	0.242	0.005	16.39	2.26
3	6.0	0.40	0.245	0.012	14.58	7.19
4	6.6	0.35	0.236	0.020	11.35	2.75
5	8.0	0.29	0.236	0.030	13.09	1.66
6	8.0	0.29	0.236	0.048	14.42	2.39
7	10.6	0.23	0.251	0.078	15.14	1.58
8	11.7	0.22	0.259	0.122	11.98	2.36
9	11.6	0.20	0.237	0.140	10.64	2.19
10	11.9	0.20	0.244	0.155	16.62	1.55
11	11.3	0.20	0.231	0.153	15.07	1.69
12	10.6	0.20	0.216	0.126	12.58	1.65
13	10.6	0.20	0.234	0.120	10.71	1.86
14	10.6	0.22	0.234	0.120	15.49	1.78
15	12.4	0.18	0.231	0.235	16.91	1.62
16	10.6	0.19	0.207	0.145	12.31	1.66
17	8.9	0.22	0.197	0.066	10.42	1.46
18	11.5	0.20	0.234	0.155	10.76	2.39
19	10.1	0.39	0.398	0.0082	8.95	2.09
20	10.1	0.35	0.364	0.0111	8.46	2.14
21	10.5	0.33	0.357	0.0137	8.14	2.15
22	11.0	0.33	0.374	0.0179	10.21	2.24
23	11.0	0.33	0.374	0.0256	11.80	2.77
24	8.6	0.24	0.208	0.054	11.33	1.56
25	11.4	0.20	0.229	0.129	11.50	1.76
26	8.8	0.24	0.215	0.046	8.37	1.89
27	10.0	0.20	0.202	0.107	11.15	1.53
28	10.0	0.18	0.183	0.105	7.89	1.45
29	10.0	0.20	0.204	0.098	9.27	1.76
30	8.3	0.20	0.167	0.049	5.74	1.36
31	11.4	0.20	0.229	0.169	13.42	1.97
32	11.2	0.19	0.216	0.164	15.71	1.41
33	15.6	0.20	0.312	0.215	11.89	2.77
34	10.2	0.18	0.183	0.121	7.29	1.65
35	10.0	0.18	0.180	0.118	8.65	1.36
36	6.7	0.22	0.153	0.051	6.66	1.97
37	7.5	0.22	0.172	0.048	6.75	1.85
38	9.2	0.74	0.694	0.0009	10.08	2.89
39	10.0	0.80	0.815	0.0006	11.28	2.43
40	10.8	0.66	0.727	0.0023	15.47	2.97
41	11.8	0.64	0.770	0.0022	16.81	2.25
42	5.9	0.23	0.140	0.048	10.68	1.38
43	10.3	0.13	0.138	0.384	7.97	1.47
44	9.4	0.14	0.134	0.280	4.82	2.32
45	9.5	0.135	0.188	0.232	6.13	1.82
46	8.3	0.154	0.127	0.190	4.55	2.20
47	7.4	0.171	0.129	0.116	5.53	1.82
48	16.5	0.175	0.294	—	20.04	—
49	15.2	0.25	0.388	—	16.59	—
50	11.0	0.13	0.142	—	7.57	—
51	9.0	0.17	0.156	—	6.87	—
52	5.0	0.44	0.224	—	19.48	—
53	—	—	0.164	—	9.12	—
54	—	—	0.212	—	9.19	—
55	—	—	0.188	—	6.03	—
56	—	—	0.153	—	6.35	—
57	—	—	0.212	—	6.87	—
58	—	—	0.279	—	13.55	—

Click on thumbnail for full-sized image.

Figures

Click on thumbnail for full-sized image.

Fig. 1. Locations of the research platforms in the Black Sea.

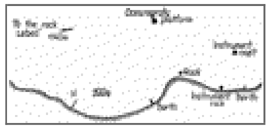

Click on thumbnail for full-sized image.

Fig. 2. Position of the nearshore research platform in Katsiveli.

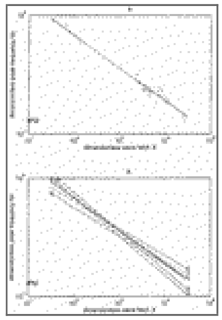

Click on thumbnail for full-sized image.

Fig. 3. (a) Dependence (8) of dimensionless peak frequency $\tilde{f}_m$ on dimensionless fetch $\tilde{X}$; (b) comparison of the dimensionless peak frequency $\tilde{f}_m$ on the dimensionless fetch $\tilde{X}$ dependency: the solid line numbered 1 is our dependence (8), dependencies numbered 2–8 are 2: JONSWAP's (1), 3: Davidan's (2), 4: Kahma's (3), 5: Donelan et al.'s (4), 6: Dobson et al.'s (5), 7: Wen's et al.'s (6), and 8: Evans and Kibblewhite's (7). PM is the Pierson–Moskowitz frequency.

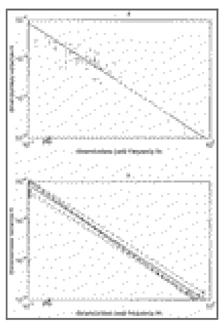

Click on thumbnail for full-sized image.

Fig. 4. (a) Dependence (10) of dimensionless wave variance $\tilde{m}$ on dimensionless peak frequency $\tilde{f}_m$; (b) comparison of the dimensionless wave variance $\tilde{m}$ on the dimensionless peak frequency $\tilde{f}_m$ dependency: the solid line numbered 1 is our dependence (10), dependencies numbered 2–8 are 2: Hasselmann et al.'s (11), 3: Davidan's (12), 4: Kahma's (13), 5: Donelan et al.'s (14), 6: Dobson et al.'s (15), 7: Wen et al.'s (16), and 8: Evans and Kibblewhite's (17). PM is the Pierson–Moskowitz frequency.

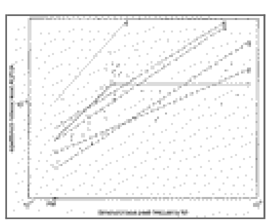

Click on thumbnail for full-sized image.

Fig. 5. Dependencies of equilibrium interval spectral density level α on dimensionless peak frequency $\tilde{f}_m$: the solid line numbered 1 is dependence (25), dependencies numbered 2–6 are 2: Donelan et al.'s (26), 3: Evans and Kibblewhite's (27), 4: Bandou et al.'s (28), 5: JONSWAP's with the laboratory data (31), and 6: JONSWAP's without the laboratory data (32). PM is the Pierson–Moskowitz frequency.

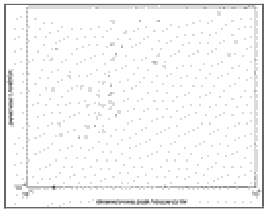

Click on thumbnail for full-sized image.

Fig. 6. Values of parameter λ (37) versus dimensionless peak frequency $\tilde{f}_m$.

Corresponding author address: Dr. Alexander V. Babanin, University College, University of New South Wales, Canberra, ACT 2600, Australia.
E-mail: a-babanin@adfa.oz.au

top